JETIR.ORG ISSN: 2349-5162 | ESTD Year : 2014 | Monthly Issue
JOURNAL OF EMERGING TECHNOLOGIES AND INNOVATIVE RESEARCH (JETIR)
An International Scholarly Open Access, Peer-reviewed, Refereed Journal

Analysis and optimization of structural and thermal behavior of modified disc brake

PRAVEEN MALVI [1], U.K. JOSHI [2]
[1]Research scholar, Department of Mechanical engineering, JEC, Jabalpur, Madhya Pradesh, India
[2]Associate Professor, Department of Mechanical engineering, JEC, Jabalpur, Madhya Pradesh, India

Abstract:

Braking systems, in the field of automotive engineering, are essential to maintaining the performance, stability, and safety of vehicles. Disc brakes are one of the most popular forms of braking mechanisms because of its effective stopping force and dependability in a variety of driving situations. Nonetheless, engineers are always looking for new and inventive methods to improve disc brake designs as part of their ongoing quest to improve vehicle performance and efficiency.

Disc brake modification offers a viable way to accomplish certain performance goals like increased durability, decreased weight, better thermal management, and improved structural integrity. Through customization of disc brake component design and materials, engineers may be able to achieve unprecedented levels of safety, lifespan, and braking efficiency.

***Key Words*: Disc brake, Heat Flux, stress, deformation, Disc profile, optimization.**

1. INTRODUTION:

This paper discusses the optimization of disc brake rotors to reduce thermal stresses and improve brake performance. The disk brake system, which acts in the axial direction, generates a significant amount of heat due to friction between brake pads and rotor faces. To maintain this temperature, the brake rotor and brake pad materials need to support the high mechanical and thermal stresses. The paper provides a useful design tool to improve the brake performance of disc brake systems.

Fig.1 ventilated disc brake and assembly.

Various studies have been conducted to analyse the thermal behaviour of solid and ventilated brake discs using ANSYS. Researchers have also investigated the thermal properties experimentally for disc brake pad systems, adjusting design variables correlated to disc brake temperature variation.
The paper also explores computational studies for determining the structural and thermal behaviours of modified disc brake rotors using SolidWorks software. The study uses five different criteria, such as temperature, heat flux, equivalent stress, deformation, and factor of safety, to design and analyse the disc brake rotor. The results provide a useful design tool for improving brake performance in disc brake systems.
In order to shed light on the performance traits and viability of such improvements, this thesis attempts to examine the structural and thermal behaviour of improved disc brakes. This project aims to address fundamental concerns about the efficiency, dependability,

and practical ramifications of altering disc braking systems through a combination of computer modelling, experimental testing, and data analysis.

This research is driven by the urgent need to expand our knowledge of how alterations affect the structural integrity and thermal management of disc brakes, especially in light of changing performance and design standards for automobiles. This study intends to make a significant contribution to the field of automotive engineering by methodically analysing the structural and thermal behaviour of modified disc brakes. This will aid in the creation

Of more reliable, effective, and creative braking solutions.

This thesis is essentially a result of a deliberate attempt to investigate the boundaries of disc brake technology, with an emphasis on comprehending and improving the thermal and structural properties of altered designs. We want to provide light on the possible advantages, difficulties, and possibilities related to changing disc brakes by meticulous study and critical inquiry, opening the door for improvements in vehicle braking systems.

2. LITTEREATURE REVIEW:

Belhocine, Ali, et al. [1] Ali Belhocine and colleagues used ANSYS to study the thermal behaviour of car brake discs. They modelled the disc brake's internal temperature distribution and identified factors affecting braking performance. They assessed stress fields and disc deformations under pad pressure using a sequentially thermal-structural linked technique. The simulations were considered satisfactory, indicating the reliability of their method in capturing the intricacies of transient heat and stress fields in disc brakes.

G. Babuyan and colleagues [2] studied thermoelastic phenomena in disk brakes using a computer model and numerical simulations. They examined temperature and contact pressure instability, focusing on carbon-carbon composites with good mechanical properties. The study advances our understanding of materials for disc brakes.

Oder et al. [3]: Oder and associates conducted a temperature and stress analysis of brake discs for railroad cars using the finite element approach. They considered two braking scenarios, centrifugal load, brake calliper holding force, and heat flow. The study provides valuable insights for designing disc brake systems, particularly for railway applications.

M.A. Malique [4] and his team developed a method for selecting materials for disc brake rotors, addressing the issue of high specific gravity in cast iron. They used digital logic and cost per unit property to analyse mechanical characteristics, and concluded that the best material was an aluminium metal matrix composite, aligning with industry trends towards lighter materials.

Daniel das et.al [5] studied the temperature and structural fields of a solid disc brake during short and emergency braking using four materials: cast iron, cast steel, aluminium, and carbon fibre reinforced plastic. The study used a finite element simulation to record temperature, friction contact power, nodal displacement, and deformation for various pressure conditions.

3. CALCULATION FOR INPUT PARAMETERS:

In the aspect of the car accident prevention, the braking performance of vehicles has been a critical issue. The rotor model heat flux is calculated for the car moving with a velocity 27.77 m/s (100kmph) and the following is the calculation procedure.

Data:

1) Mass of the vehicle = 2500 kg
2) Initial velocity (u) = 27.7 m/s (100 kmph)
3) Vehicle speed at the end of the braking application (v) = 0 m/s
4) Brake rotor diameter = 0.262 m
5) Axle weight distribution 30% on each side (γ)=0.3
6) Percentage of kinetic energy that disc absorbs (90%) k=0.9
7) acceleration due to gravity g =9.81m/s2
8) coefficient of friction for dry pavement μ=0.7

Kinetic energy is defined by the equation [9]

(a) Energy generated during braking

K. E= $k\ ½\ \Upsilon \frac{m(u-v)^2}{2}$ = **129465.3 J**

(b) To calculate stopping distance

$d = \frac{u^2}{2\mu g}$ = **56.18 m**

(c) To calculate deceleration time

$v = u + at$

Deceleration time = Braking time = 4s

(d) Braking Power: Braking power during continued braking is obtained by differentiating energy with respect to time.

P_b = K.E/ t = **32366.25 W**

(e) Calculate the Heat Flux (Q): Heat Flux is defined as the amount of heat transferred per unit area per unit time, from or to a surface.

Q=P_b/A = **1201084.422 W/m²**

I. ANALYTICAL TEMPERATURE RISE CALCULATIONS:

The contact area between the pads and disc of brake components, heat is generated due to friction. For calculation of heat generation at the interface of these two sliding bodies, two methods are suggested on the basis of “law of conservation of energy which states that the kinetic energy of the vehicle during motion is equal to the dissipated heat after vehicle stop” [7]. The material properties and parameters adopted in the calculations are as shown in table1 [9].

Table.1 Material Properties for Stainless Steel and Cast Iron.

Material Properties.	**Stainless Steel (Model I)**	**Cast Iron (Model II)**
Thermal conductivity (w/m k).	36	50
Density, ρ(kg/m³)	7100	6600
Specific heat, c (J/Kg ˚C)	320	380
Thermal expansion, α ($10^{-6}/k$)	0.12	0.15
Elastic modulus, *E* (GPa)	210	110
Coefficient of friction, μ	0.5	0.5
heat transfer coefficient h(w/km²)	150	120
Operation Conditions	**Operation Conditions**	**Operation Conditions**
Angular velocity, (rad /s)	50	50
Braking Time Sec	4	6
Hydraulic pressure, *P* (Mpa)	1	1

Single stop temperature rise T_{max} is the temperature rise due to single braking condition.

$$T_{max} = 0.5278 \text{ x } q \text{ x } \frac{\sqrt{t}}{\sqrt{p.c.k}} + T_{max}$$

The relative brake temperature after the n^{th} brake application can be calculated using relation,

$$T_{roa} - T_i = \frac{\left[1-e^{\frac{-nhAt_C}{\rho cv}}\right][\Delta t]}{1-e^{(-hAt_C)/(\rho cv)}}$$

The compressive stresses 'σ'developed in the surface of a disc from sudden temperature increases is

$$\sigma = \frac{E}{1-\nu} \text{ X } \alpha \text{ X } \Delta t$$

II. FINITE ELEMENT ANALYSIS:

The finite element method has become a powerful tool for the numerical solutions of a wide range of engineering problems. It has been developed simultaneously with the increasing use of the high- speed electronic digital computers and with the growing emphasis on numerical methods for engineering analysis. In this step it defines the analysis type and options, apply loads and initiate the finite element solution. This involves three phases:

- Pre-processor phase
- Solution phase
- Post-processor phase

The ANSYS Workbench, together with the Workbench projects and tabs, provides a unified working environment for developing and managing a variety of CAE information and makes it easier for set up and work with data at a high level. Workbench includes the following modules "ANSYS Design Space" is referred to as Simulation "ANSYS AGP" is referred to as Design Modeler and "ANSYS Design explorer" referred to as Design explorer. Workbench provides enhanced interoperability and control over the flow of information between these task modules. Various tools and techniques are incorporated for efficiently manage to large models. Like tree filtering tagging tree Objects, connections worksheet, object generator, submodeling. Data can be transferred from a 2D coarse model [Full Model] to a 3D sub model. Submodeling is available for structural and thermal analysis types with solid geometry.

a) FEM Model of Solid Disc and Ventilated Disc Brake.

The finite element model of disc brake constructed for the dimensions as shown in fig.2 the inner radius, outer radius and flange thicknesses of discs are as 0.08, 0.0131 and 0.024m for cast iron and stainless steel respectively to both cases solid and ventilated disc.

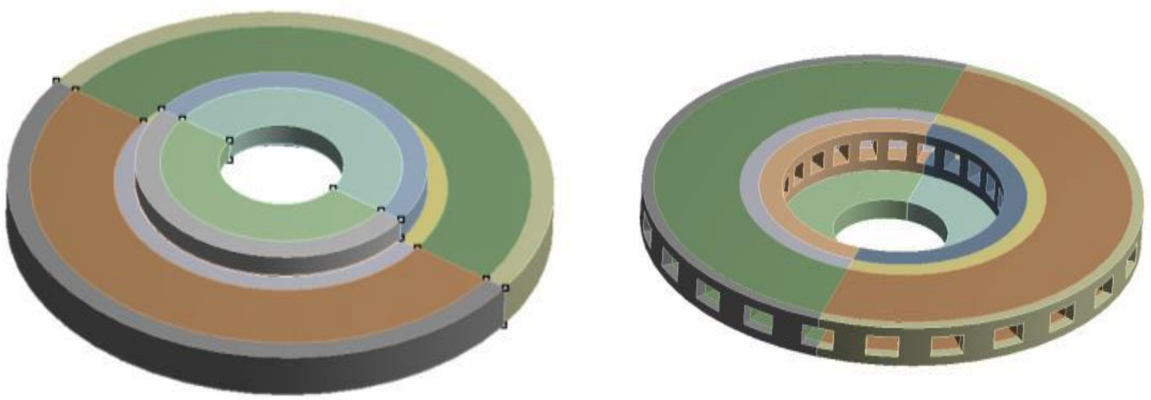

(a) Case I (b) Case II

Fig.2 FEM model of 24mm solid Disc Brake (a) and ventilated disc (b) of both cast iron and stainless-steel discs.

b) Meshing Details.

The goal of meshing in Workbench is to provide robust, easy to use meshing tools that will simplify the mesh generation process. The model using must be divided into a number of small pieces known as finite elements. Since the model is divided into a number of discrete parts, in simple terms, a mathematical net or "mesh" is required to carry out a finite element analysis. A finite element mesh model generated is shown in fig.3.The mesh results are as shown in table No 2. The elements used for the mesh of the model are tetrahedral three-dimensional elements with 8 nodes.

Table.2 Details of Mesh Model.

Models	Material Type	Number of Elements	Number of Nodes
Solid Disc (case I)	Cast iron	8680	40935
	Stainless steel		
Ventilated disc	cast iron	55426	112171

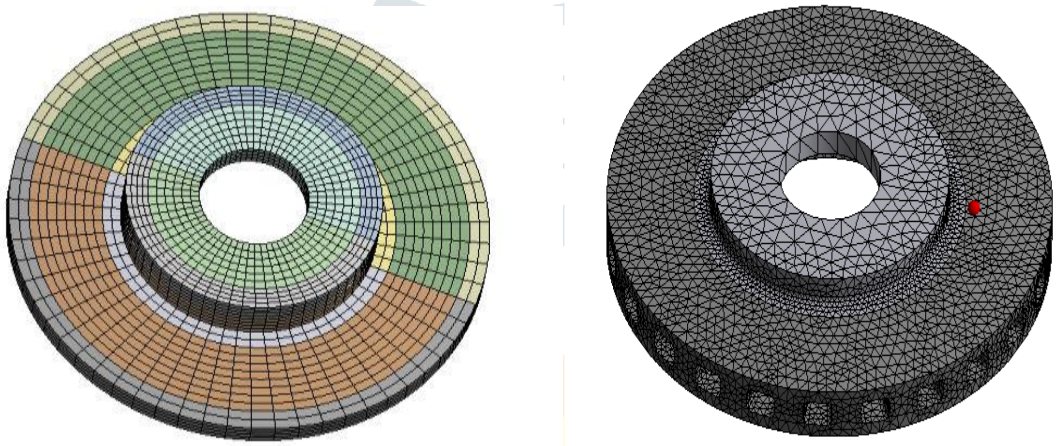

Fig.3 FEA Model Mesh Model for solid disc and ventilated disc.

c) Thermal and Structural Boundary Conditions.

The boundary conditions are introduced into module ANSYS Workbench, by choosing the mode of simulation and by defining the physical properties of materials and the initial conditions of simulation. In this work, a transient thermal analysis will be carried out to investigate the temperature variation across the both disc by applying heat flux value for repeated braking applications using ANSYS. Further structural analysis is carried out by coupling thermal analysis. In addition, convection heat transfer coefficient is applied at the surface of the ventilated disc for the analysis as shown in fig 4.

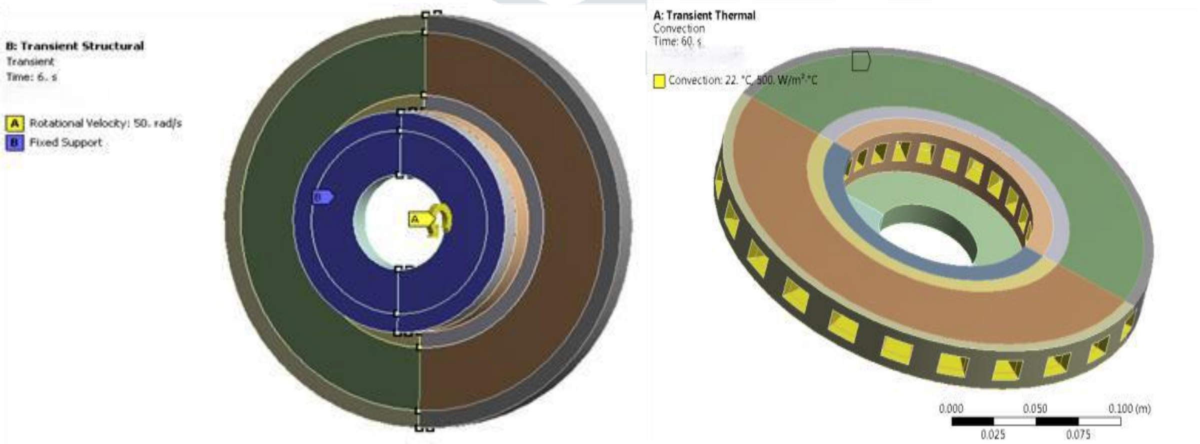

Fig.4 Thermal and Structural Boundary Conditions for solid and ventilated disc

4. RESULTS AND DISCUSSIONS:

To validate the present models, a transient thermal analysis behaviour of disc brake was performed for the operating condition of the constant hydraulic pressure P =1Mpa and angular velocity ω = 50 rad/s (drag brake application) during 10 seconds. The ANSYS simulation is obtained in 6 repeated brake applications. One cycle is composed of braking time of 4sec and constant speed driving. The time step Δt =0.001 sec was used in the computations. In each process, the heat flux distribution on the friction surfaces after time t=4 sec does scarcely occur and then the steady state is reached. The hydraulic pressure was assumed to linearly increase to 1MPa by 1.5 sec and then kept constant until 4sec. Also, the angular velocity was assumed to decay linearly and finally become zero at 4sec. The results obtained from analytical and FEM solutions are compared for both transient thermal and structural behaviour of the model. Finally, the best model is suggested. In addition, based on disc brake performance a ventilated radial vanes disc brake analysis of two different materials is carried out for 6 braking conditions. Comparisons of solid discs case I and ventilated discs case II are performed to validate the results.

CASE I: Solid Disc.

1.Stainless Steel Temperature Results.

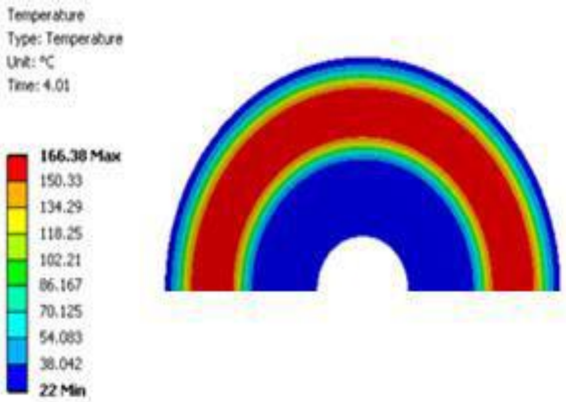

Fig.5 SS Disc 1st Braking Temperature Contours.

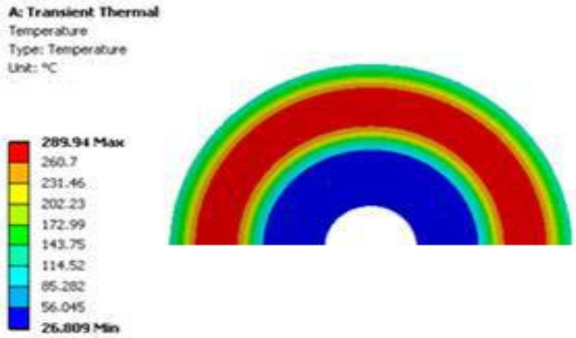

Fig.6 SS Disc 3rd Braking Temperature Contours.

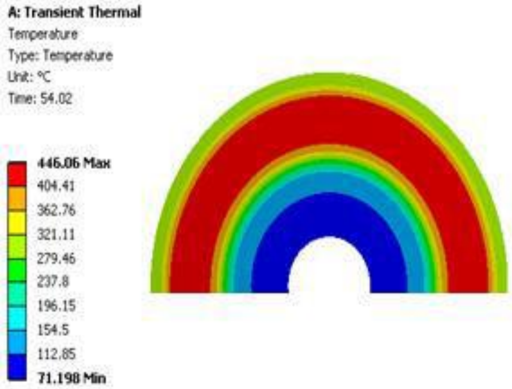

Fig.7 SS Disc 6th Braking Temperature Contours.

2.Cast Iron Temperature Results.

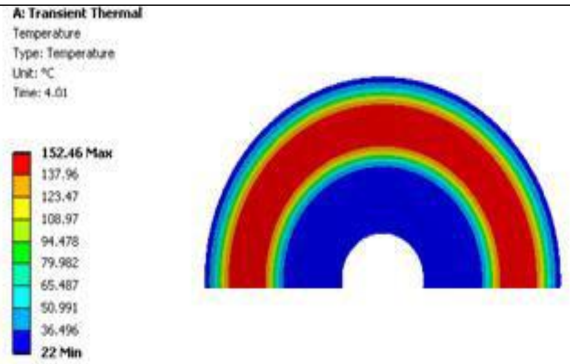

Fig.8 C I Disc 1st Braking Temperature Contours.

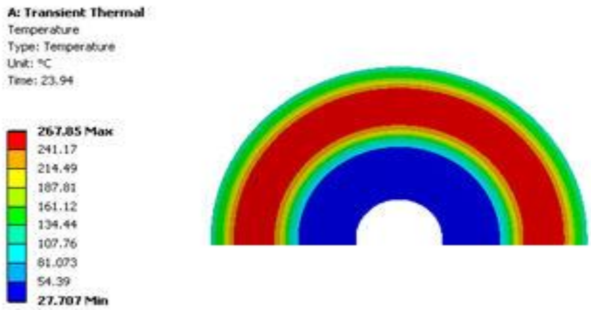

Fig.9 C I Disc 3rd Braking Temperature Contours.

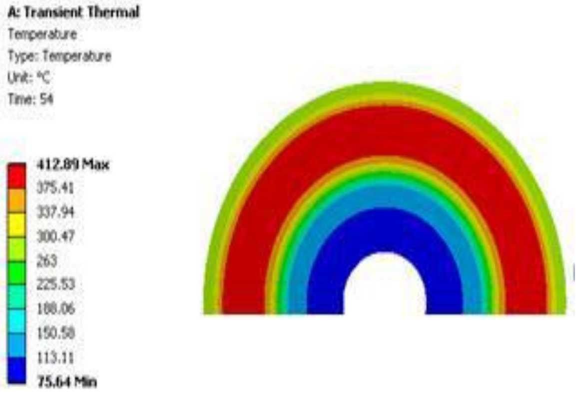

Fig.10 C I Disc 6th Braking Temperature Contours.

During each braking cycle, the temperature on surface of the disc is raises. During 1st braking, the temperature rises from ambient temperature 22 ˚C to 166 ˚C. Similarly for alternate braking applications, during 3rd braking and 6th breaking it rises to 289 ˚C and 446 ˚C for solid stainless-steel disc respectively. Similarly in the cast iron solid disc 1st, 3rd and 6th braking applications the temperature rise is 152 ˚C, 267 ˚C and 412 ˚C respectively. The maximum temperature rise is indicated in red colour and green colour shows average temperature rise at the friction surface around the circumference of the disc as shown in figures 5,6,7,8,9,10.

<table>
<tr><th>Stainless Steel Deformation and Stress Contours.</th><th>Cast Iron Deformation and Stress Contours.</th></tr>
<tr><td>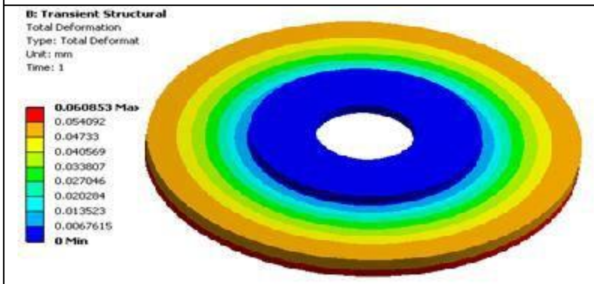

Fig.11 stainless steel Brake Deformation Contours.</td><td>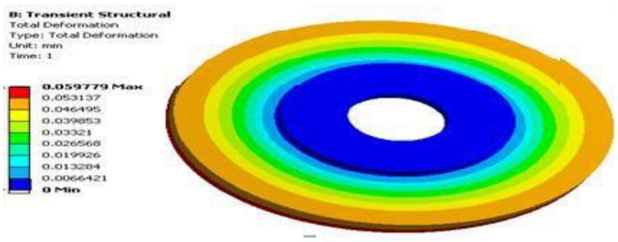

Fig.13 Cast Iron Brake Deformation Contours.</td></tr>
<tr><td>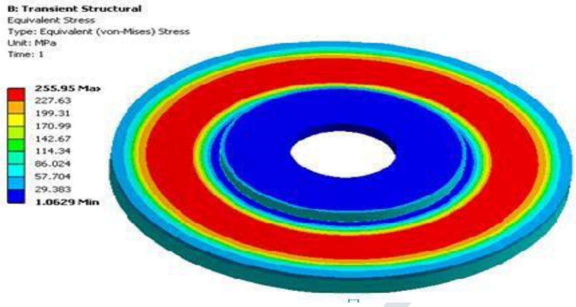

Fig.12 stainless steel Brake Von Misses Contours.</td><td>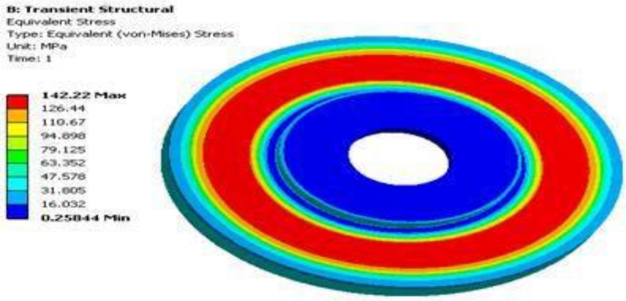

Fig.14 Cast Iron Brake Von Misses Contours.</td></tr>
</table>

The distribution of the total distortion in solid stainless-steel cast-iron disc brake is shown in fig11. The scale of values of the deformation varies from 0 µm with 0.06mm which corresponds to the time of braking. After the 6th braking, the maximum deflection induced is 0.0608mm in SS disc and 0.059 in C I disc, which is less than the allowable deflection 0.5mm. During the total time simulation of braking for a full disc presents the distribution of the constraint equivalent of Von Mises Stresses to various moments of simulation as shown in fig12. The scale of values varies from 0 MPa to 255MPa in stainless steel disc and 142 MPa in cast iron disc, which is the maximum thermal stress induced at maximum temperature rise after 6th braking application.

Case II: Ventilated Disc.

<table>
<tr><th>1.Stainless Steel Temperature Results.</th><th>2.Cast Iron Temperature Results.</th></tr>
<tr><td>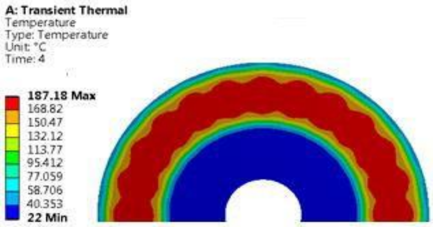

Fig.15 SS Disc 1st Braking Temperature Contours.</td><td>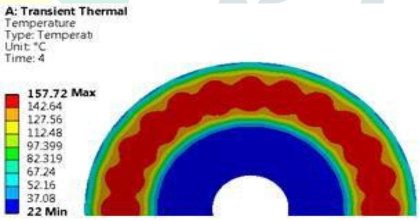

Fig.18 C I Disc 1st Braking Temperature Contours.</td></tr>
<tr><td>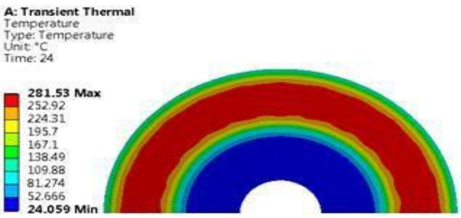

Fig.16 SS Disc 3rd Braking Temperature Contours.</td><td>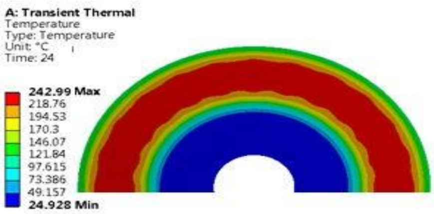

Fig.19 C I Disc 3rd Braking Temperature Contours.</td></tr>
</table>

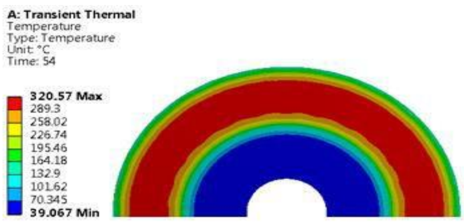

Fig.17 SS Disc 6th Braking Temperature Contours.

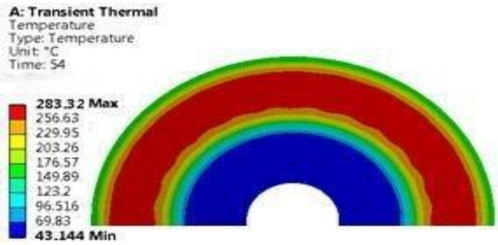

Fig.20 C I Disc 6th Braking Temperature Contours.

During each braking cycle, the temperature on surface of the disc is raises. During 1st braking, the temperature rises from ambient temperature 22 ˚C to 187 ˚C. Similarly for alternate braking applications, during 3rd braking and 6th breaking it rises to 281 ˚C and 320 ˚C for solid stainless-steel disc respectively. Similarly in the cast iron solid disc 1st, 3rd and 6th braking applications the temperature rise is 157 ˚C, 242 ˚C and 283 ˚C respectively. The maximum temperature rise is indicated in red colour and green colour shows average temperature rise at the friction surface around the circumference of the disc as shown in figures15,16,17,18,19,20.

Stainless Steel Deformation and Stress Contours.	Cast Iron Deformation and Stress Contours.

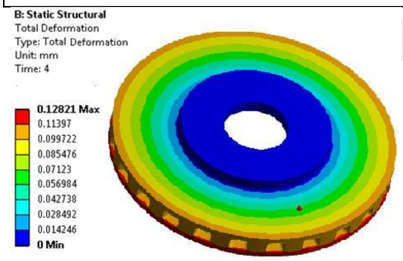

Fig.21stainless steel Brake Deformation Contours.

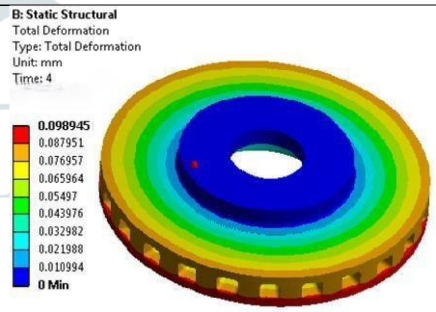

Fig.23 Cast Iron Brake Deformation Contours.

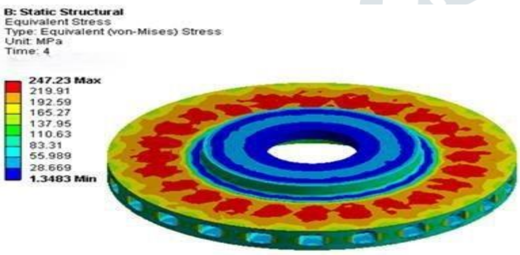

Fig.22stainless steel Brake Von Misses Contours.

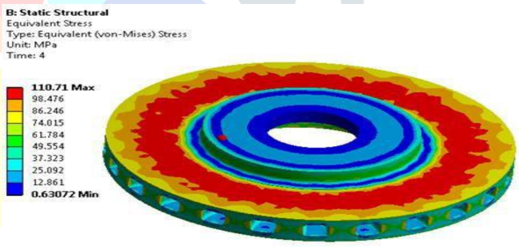

Fig.24 Cast Iron Brake Von Misses Contours.

The distribution of the total distortion in stainless steel and cast-iron ventilated disc brake is shown in fig21. The scale of values of the deformation varies from 0 µm to 0.0128mm and which corresponds to the time of braking. After the 6th braking, the maximum deflection induced is 0.0128mm in SS ventilated disc and 0.098mm in C I ventilated disc, which is less than the allowable deflection 0.5mm. The distribution of the constraint equivalent of Von Mises Stresses The scale of values varies from 0 MPa to 288MPa for in stainless steel disc and 110 MPa in cast iron disc. Which is the maximum thermal stress induced at maximum temperature rise 320 ˚C and 283 ˚C after 6th braking application respectively.

5. COMPARISON THE RESULTS OF SOLID AND VENTILATED DISC.

Table.3 Comparison the Results of Solid and Ventilated Disc.

S.no.	Material Flange width (mm)	Analytical Max. Temp. ˚C	FEM Max. Temp. ˚C	Deflection in (mm)	Analytical misses stress (Mpa)	FEM Von miss's stress (Mpa)
	Solid Brake					
1	SS 24	464	446	0.0608	270	256
2	CI 24	425	413	0.0590	160	142

Ventilated Disc Brake						
1	SS	340	321	0.105	186	247
2	CI	308	283	0.098	99	110

Comparing the different results of temperature rise, deflection, and stress field obtained from analysis it shows that the ventilated cast iron disc has reduction in temperature, deflection and stresses. It is concluded that ventilated type cast iron disk brake is the best for the present application.

6. CONCLUSIONS:

I. Comparing the different results of temperature rise, deflection, and stress field obtained from analysis it shows that in the ventilated cast iron disc reduction in temperature, stresses and deformation by 31.43% , 22.3% and 8% respectively than the solid disc.

II. It is concluded that ventilated type disk brake is the best for the present application. All the values obtained from the analysis are less than their allowable values. Hence the brake disk design is safe based on the strength and rigidity criteria.

7. REFERENCES:

[1] Ali Belhocine, Mostafa Bouchetara Thermo- mechanical modelling of dry contacts in automotive disc brake at International Journal of Thermal Sciences 60 (2012) 161e170, 2012 Published by Elsevier Masson SAS. Sciences 60 (2012) 161e170, 2012 Published by Elsevier Masson SAS.

[2] G. Babukanth and M. Vimal Teja Transient Analysis of Disk Brake By using Ansys Software International Journal of Mechanical and Industrial Engineering (IJMIE), ISSN No. 2231 –6477, Vol-2, Issue-1, 2012.

[3] Oder, G., Reibenschuh, M., Lerher, T., Sraml, M.; Samec, B.; Potrc, I. Thermal and Stress Analysis of Brake Discs in Railway Vehicles at International Journal of Advanced Engineering 3(2009)1, ISSN 1846-5900.

[4] Daniel Das. A, Christo Reegan Raj.V, Preethy.S, Ramya Bharani.G Structural and Thermal Analysis of Disc Brake in Automobiles at International Journal of Latest Trends in Engineering and Technology (IJLTET) ISSN: 2278-621X Vol. 2 Issue 3 May 2013.

[5] M.A. Maleque, S. Dyuti and M.M. Rahman (Member, IAENG). Material Selection Method in Design of Automotive Brake Disc at Proceedings of the World Congress on Engineering 2010 ISBN: 978-988-18210-8-9 ISSN: 2078-0958 (Print); ISSN: 2078-0966 (Online) Vol III WCE 2010, June 30 - July 2, 2010, London, U.K.

6] M.J. Han, Jae, coupled thermo-mechanical analysis and shape optimization for reducing uneven wear of brake pads, Int. Automotive Technol. 18 (2017) 1027–1035.

[7] S. Ahmed, G. Mohammed, S. Agarin, Design, development and FE thermal analysis of a radially grooved brake disc developed through direct metal laser sintering, Materials 11 (2018) 1211.

[8] R.S. Kajabe, R.R. Natvar, Optimization of Disc Brake Rotor with Modified Shape, International Journal of Research in Aeronautical and Mechanical, Engineering 3 (2015) 52–60.

[9] G. Pan, R. Cai, Thermal Stress Coupling Analysis of Ventilated Disc Brake Based on Moving Heat Source, Adv. Mater. Sci.Eng. 2018 (2018).

[10] T. Babu, R. Sudharshan, R. Akil, S. Chiranjeev, Analysis and Shape Optimization of disc Brake with Alternate, Material 8 (2019) 187–192.

[11] I. Mahariq, M. Kavyanpoor, M. Ghalandari, M.A. Nazari, D.T. Bui, Identification of nonlinear model for rotary high aspect ratio flexible blade using free vibration response, Alexandria Eng. J. 59 (2020) 2131–2139.

[12] T. Abdeljawad, I. Mahariq, M. Kavyanpoor, M. Ghalandari, N. Nabipour, Identification of nonlinear normal modes for a highly flexible beam, Alexandria Eng. J. 59 (2020) 2419.

[13] I. Mahariq, A. Erciyas, A spectral element method for the solution of magnetostatic fields, Turk. J. Electr. Eng. Comput. Sci. 25 (2017) 2922–2932.

[14] I. Mahariq, H. Kurt, M. Kuzuoglu, questioning degree of accuracy offered by the spectral element method in computational electromagnetics, Appl. Comput. Electromagnet. Soc. J. 30 (2015) 698–705.

[15] I. Mahariq, On the application of the spectral element method in electromagnetic problems involving domain decomposition, Turk. J. Electr. Eng. Comput. Sci. 25 (2017) 1059–1069.

[16] I. Mahariq, M. Kuzuolu, I.H. Tarman, H. Kurt, Photonic nanojet analysis by spectral element method, IEEE Photonics J.6 (2014) 6802714.

[17] I. Mahariq, M. Kuzuolu, H. Tarman, On the Attenuation of the Perfectly Matched Layer in Electromagnetic Scattering Problems with the Spectral Element Method, ACES J. 29(2014) 701.

[18] I. Mahariq, H. Kurt, Strong field enhancement of resonance modes in dielectric microcylinders, J. Opt. Soc. Am. B 33 (2016)656–662.

[19] I. Mahariq, H. Tarman, M. Kuzuolu, On the Accuracy of Spectral Element Method in Electromagnetic Scattering Problems, Int. J. Comput. Theory Eng. 6 (2014) 495–499.

[20] https:/www.alibaba.comproduct-detailCompetitive-Price-brake-disc 220mmmotorcycle_60044723228.html.

[21] Tadeusz Stolarski, Yuji Nakasone, Shigeka Yoshimoto, Engineering analysis with ANSYS software, Butterworth-Heinemann, 2018.

[22] Y.H. Mishra, V.R. Deulgaonkar, P.A. Makasare, Design and Optimization of Disc Brake Rotor (For Two-Wheeler), Int. Eng.Res. J. (2015) 288–300.